Remote Sensing of Three–Dimensional Inhomogeneous Cirrus Clouds: Application to Climate Research

K. N. Liou, S. C. Ou, P. Rolland, and Y. Gu

Department of Atmospheric Sciences, University of California, Los Angeles, California

G. Mace and K. Sassen

Department of Meteorology, University of Utah, Salt Lake City, Utah

ABSTRACT

We have innovated a remote sensing technology involving the construction of a three-dimensional field of the ice water content and ice crystal mean size of cirrus clouds in space and time based on a combination of satellite and ground–based mm–wave cloud profiling radar observations. We demonstrate the importance of the three–dimensional inhomogeneous cloud field determined from remote sensing for the development of a physically–based cloud–radiation parameterization for climate research.

1. Introduction

Cirrus clouds are globally distributed, being present at all latitudes and in all seasons with a global cloud cover of about 20-30% and more than 70% in the tropics (Wylie et al. 1994). The effects of cirrus clouds on the radiation budget of the earth and the atmosphere, and hence, their impact on weather and climate processes, have been articulated by Liou (1986, 1992). Satellite mapping of the optical depth in midlatitude and tropical regions has illustrated that cirrus clouds are frequently finite in nature and display substantial horizontal variabilities. Vertical inhomogeneity of the ice crystal size distribution and ice water content has also been demonstrated in balloon–borne replicator sounding observations, as well as time series of backscattering coefficients derived from lidar returns. However, methodology for the mapping of three–dimensional (3D) inhomogeneous clouds in space and time has not been developed at this point.

Radiative heating drives the dynamic and thermodynamic processes in the atmosphere. Radiative equilibrium at the top of the atmosphere represents the first approximation for climate. Since radiative heating is strongly regulated by clouds, knowledge and understanding of the optical and microphysical properties of cirrus clouds are essential for the development of radiation parameterizations for incorporation in climate models. A physically–based radiation parameterization for cirrus clouds and their radiative properties for use in climate models must account for the finite and inhomogeneous nature of these clouds in 3D space.

We have innovated a remote sensing methodology for the retrieval of ice water content (IWC) and ice crystal mean size (DE) of cirrus in 3D space based on a unification of satellite and ground–based mm–wave cloud profiling radar (mmCR) observations. We first present the conceptual approach of 3D remote sensing, followed by its application to climate research.

2. Conceptual Approach to Three–Dimensional Remote Sensing

a. *Satellite Remote Sensing*

Recent advances in satellite remote sensing of cirrus clouds have demonstrated that their optical depth and mean effective ice crystal size, as defined in Liou et al. (1998), can be retrieved from the operational NOAA AVHRR channels and the MODIS channels on board the NASA EOS/TERRA satellite launched in December 1999. Ou et al. (1995, 1996) have used a thermal infrared technique based on the thermal component of 3.7 μm and 10.9 μm to infer cirrus cloud optical depth and mean effective ice crystal size using AVHRR data collected during FIRE–I and FIRE –II IFO. Using SUCCESS and CEPAX MAS (MODIS Airborne Simulator) data, Rolland and Liou (2000) have shown that cirrus optical depth and mean effective ice crystal size can be determined from correlations of 0.63/1/6 and 0.63/2.13 μm wavelengths. Neither the 1.6 μm nor the 2.13 μm channel is available on the operational satellites at present. Our recent work in this area (Ou et al. 1999)

Corresponding author address: Prof. K. N. Liou, Department of Atmospheric Sciences, University of California, Los Angeles, 405 Hilgard Ave., Los Angeles, CA 90095. E-mail: knliou@atmos.ucla.edu

shows that the correlation approach can be applied to the AVHRR 0.63 μm and 3.7 μm (total radiance) channels to infer cirrus cloud optical depth and mean effective ice crystal size.

In Fig. 1a, we demonstrate the basic principle of the two–channel correlation technique for the retrieval. Six ice crystal size distributions in terms of the mean effective ice crystal sizes and two mean effective water droplet radii were used along with optical depths ranging from 0.5 to 64 to perform radiative transfer simulations to obtain 2D reflectance diagrams. The visible reflectance mainly depends on the optical depth, whereas the near IR reflectances are primarily functions of the mean effective particle size. Also shown are MAS data obtained from FIRE–II IFO on 5 December 1991. The case over water was taken at 1636 UTC when ER–2 was flying over the northern part of the Gulf of Mexico near the southern coastal region of Louisiana. The case over land was taken at 1923 UTC when ER–2 was flying over eastern Oklahoma. The data points suggest that the detected cirrus appears to contain small ice particles with optical depths less than 3. Larger optical depth indicates the possibility of cirrus overlying low clouds. Collocated in–situ microphysics data were not available for validation in these cases, however. Fig. 1b displays a similar correlation diagram for the 0.63 μm reflectance and 3.7 μm radiance (total). Overlapped with the curves are NOAA–11 AVHRR data for a 0.05° × 0.2° area near the balloon launch site where ice crystal size distribution was measured by balloon–borne replicators. Fig. 1c shows comparison of the five carefully selected cases of retrieval results from the 0.63/3.7 μm correlation technique with those from in–situ analyses. The cases of single– and multi–layer cirrus clouds are denoted in the diagram. The satellite–retrieved optical depths are within about 10% of the in–situ values, while the retrieval mean effective ice crystal sizes are within about 5 μm of the in–situ values.

b. Ground–Based mm–Wave Radar and Lidar Backscattering

Under the sponsorship of the DOE Atmospheric Radiation Measurement (ARM) program, Mace et al. (1998) and Mace (1999, personal communication) have developed a technique for the retrieval of the IWC and ice crystal size of cirrus clouds by employing a combination of reflectivity and Doppler velocity and spectral width of the 33 GHz Doppler radar. In this approach, the ice crystal size distribution is assumed to conform to a modified gamma distribution consisting of hexagonal columns from which the Rayleigh–Gans theory is used to model the backscatter and estimate the fall velocity. A look–up table is constructed based on which retrievals of the cloud parameters can be carried out from radar backscatter data.

Fig. 2a displays the time series of the retrieved IWC and ice crystal length as functions of height for the 26 September 1997 Hurricane Nora cirrus cloud case observed at the SGP CART site. This cirrus cloud varied from about 1 to 3 km over a time period of 6 hours and substantial variabilities in both IWC and ice crystal size in the vertical are shown. Note that the vertical resolution of the mm radar is about 90 m. Preliminary validation of the retrieval algorithm has also been made by using the ice crystal size distribution measured by the 2DC probe on board the University of North Dakota Citation.

Although a direct inference of IWC and ice crystal size from lidar backscatter returns has yet to be developed, lidar can provide accurate cirrus cloud vertical and horizontal boundaries as well as extinction coefficient profiles (Sassen 1991). Demonstrated in Fig. 2b is a backscatter image from a 0.532 μm lidar corresponding to the 33 GHz radar data presented in Fig. 2a, except the UTC time is only up to 2100. The cloud thickness is clearly defined in the lidar backscattering return.

c. Unification of Satellite and mm–Wave Radar Data

To construct 3D IWC and ice crystal size fields from satellite/radar/lidar data, let the optical depth and mean effective size retrieved from satellite data be denoted by $\tau(x, y)$ and $DE(x,y)$, respectively. Note that the AVHRR–HRPT data have a horizontal resolution of about 1 km by 1 km at nadir. From the mmCR backscatter retrieval described above, IWC(x,z) and DE(x,y) can be determined. The vertical optical depth is a function of the ice water path (IWP), which is the product of IWC, cloud thickness Δz, and mean effective ice crystal size, representing the ice crystal size distribution. In the limits of geometric optics applicable to solar wavelengths (Liou 1992, p 308), we have

$$\tau(\lambda;x,y) \cong \mathrm{IWC}(x,y)\,\Delta z\,(x,y)[a_0(\lambda) + a_1(\lambda)/\mathrm{DE}(x,y)] \quad (1)$$

where a_0 and a_1 are spectral coefficients that can be determined from "exact" calculations *a priori* and $\Delta z(x)$ can be determined from lidar backscattering. Variation of Δz along the y–direction may be assumed to be small as compared to that along the x–direction. Thus, the satellite–retrieved $\tau(x, y)$ and $DE(x, y)$ can be used to infer IWC (x, y).

Next, from the IWC and DE determined from radar, and again assuming their variabilities along the y–direction are relatively small in comparison with those along the x–direction, we can derive normalized values of $\mathrm{IWC}^*(x,z) = \mathrm{IWC}(x,z)/\overline{\mathrm{IWC}(x)}$ and $\mathrm{DE}^*(x,y) = \mathrm{DE}^*(x,y) / \overline{\mathrm{DE}(x)}$, where the bar terms are averaged values along the vertical direction. It follows that the 3D fields can be determined from the following:

$$\mathrm{IWC}\,(x, y, z) = \mathrm{IWC}\,(x, y) \cdot \mathrm{IWC}^*(x, z), \quad (2a)$$

$$\mathrm{DE}\,(x, y, z) = \mathrm{DE}(x, y) \cdot \mathrm{DE}^*(x, y). \quad (2b)$$

Moreover, the extinction coefficient profile determined from lidar backscattering can further be used to cross check the optical depth parameterization denoted in Eq.

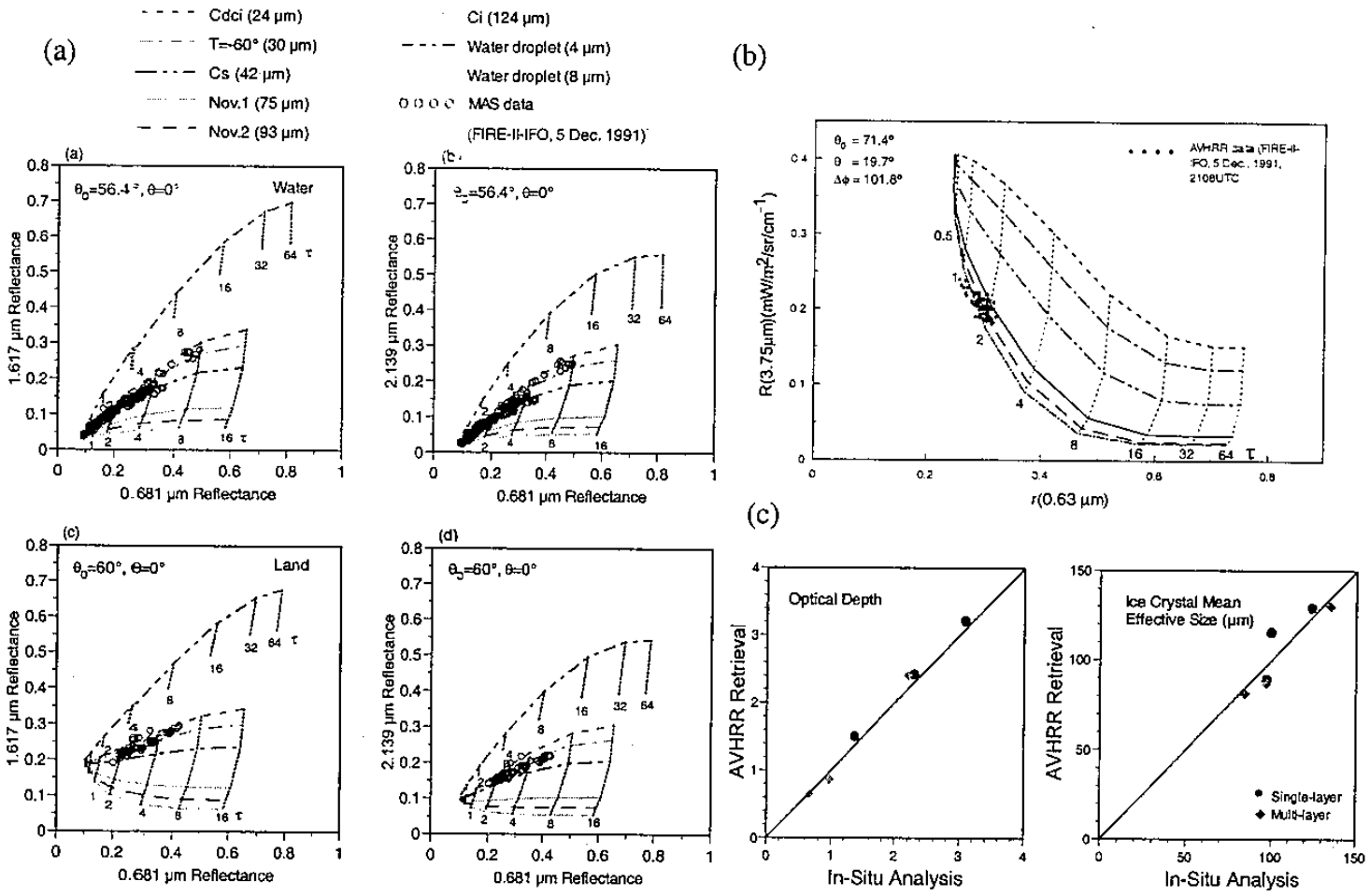

Fig.1. (a) Display of the MAS data gathered from FIRE II IFO on 5 December 1991 over both land and water surfaces in 0.681/2.139 mm 2D correlation diagrams for six mean effective ice crystal sizes and two mean effective water droplet radii covering the optical depths from 0.5 to 64. (b) Display of the AVHRR data collected on the same date in the 2D correlation diagram for 0.63 mm reflectance and 3.7 mm total radiance. (c) Comparison of five cases of retrieval results from the 0.63-3.7 μm correlation technique with those from in-situ analyses. Also shown is the comparison of six cases of results from a IR retrieval technique with in-situ analyses.

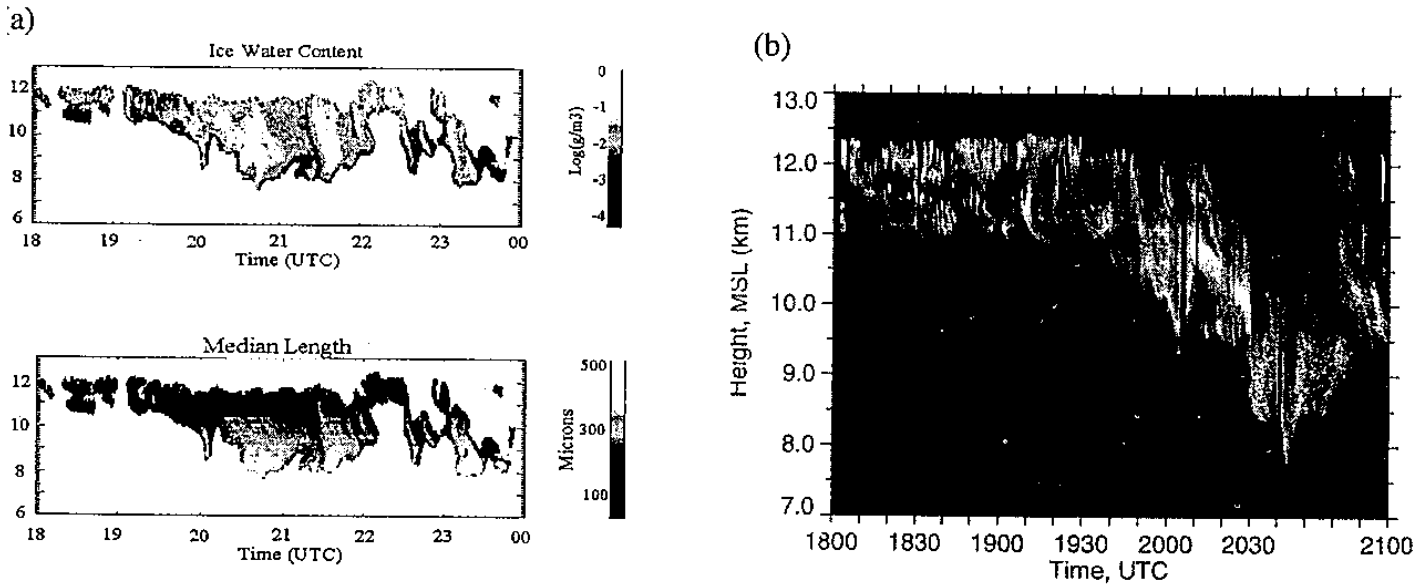

Fig. 2. (a) Time series of the IWC and ice crystal length profiles retrieved from the 33mm radar for the 26 September 1997 Hurricane Nora cirrus cloud case observed at the SGP CART site (Mace 1999). (b) Backscatter image from a 0.532 mm lidar corresponding to the 33GHz radar presented in (a) (Sassen 1999).

(1). The 3D IWC and DE fields so constructed will have the satellite (~ 1 km × 1 km horizontal) and radar (~70 m vertical) resolutions.

We have selected collocated and coincident AVHRR/NOAA and DOE/ARM mmCR data gathered at the CART site in the northern Oklahoma areas involving single cirrus and cirrus over low stratus during three ARM IOPs in the Spring of 1997 to test our methodology. Retrieval and analysis will be carried out to construct 3D IWC and DE fields, and assessed with collocated in–situ measurements of the ice crystal size distribution and IWC independently derived from optical probes on board the University of North Dakota Citation. The MODIS data from TERRA/EOS will also be used for this study if it becomes available in time.

3. Application to Climate Research and Discussion

The link between cloud/radiation parameterizations and the development and perfection of GCMs is indeed intricate and nonlinear, since the success of climate predictions depends on many other physical processes. At present, prediction of clouds in GCMs is still rudimentary. Most of the models now have the prognostic prediction equations for ice/liquid water content. However, cloudiness (or cloud cover) prediction has been and still is based on empirical parameterization employing large–scale relative humidity (Liou and Zheng, 1984; Liou, 1992; Xu and Krueger 1991) and cloud water mixing ratio (Randall et al. 1996). Parameterization of the cloud inhomogeneity that has been observed by satellites and ground–based radar and lidar as discussed in Section 2 is a subject still in its embryonic stage. However, cloud inhomogeneity must be included in the future generation of GCMs based on fundamental subgrid turbulence theory (Arakawa, personal communication).

Radiative heating in the atmosphere is strongly regulated by clouds. Thus, any cloud parameterization developed must be tested in connection with radiative flux and heating rate calculations to ensure its physical reliability and consistency. A physically–based radiation parameterization can provide an off–line investigation and insight towards understanding the response of cloud conditions to radiative fluxes and heating rates. In the following, we demonstrate the manner in which 3D cloud remote sensing products can be incorporated in a radiative transfer parameterization model.

From the retrieved IWC and DE values, we wish to determine the single–scattering properties of 3D cloud fields. We shall follow the parameterization approach developed by Fu and Liou (1993). In this approach, the extinction coefficient, single–scattering albedo, and asymmetry factor, which are functions of the position vector and wavelength, can be parameterized in terms of IWC and DE as follows:

$$\beta_e(\lambda;x,y,z) = \mathrm{IWC}(x,y,z)\sum_{n=0}^{N} a_n(\lambda)/\mathrm{DE}^n(x,y,z), \qquad (3a)$$

$$1-\varpi(\lambda;x,y,z) = \sum_{n=0}^{N} b_n(\lambda)\mathrm{DE}^n(x,y,z), \qquad (3b)$$

$$g(\lambda;x,y,z) = \sum_{n=0}^{N} c_n(\lambda)\mathrm{DE}^n(x,y,z), \qquad (3c)$$

where a_n, b_n, and c_n are certain coefficients that must be determined from numerical fitting based on "exact" light scattering and absorption calculations for a range of ice crystal size distributions and shapes. Fu and Liou (1993) have found that N = 1–2 is sufficient in these parameterizations to achieve an accuracy within 1% in the fitting. Once the 3D spectral single–scattering properties are defined, we may incorporate them in a radiative parameterization program that has been developed for 3D inhomogeneous cloud fields (Gu and Liou 2000a,b). Flux and heating rate profiles can subsequently be evaluated as functions of the spatial coordinates (x, y, z). Although our prime application is for cirrus clouds, the conceptual approach of parameterization should be applicable to general cloud fields as well.

Our radiation parameterization utilizes a diffusion approximation approach for application to inhomogeneous media employing Cartesian coordinates. The extinction coefficient, single–scattering albedo, and asymmetry factor are functions of spatial position and wavelength and are parameterized in terms of IWC and DE as defined above. We employ the correlated k–distribution method for incorporation of gaseous absorption in multiple scattering atmospheres. Delta–function adjustment is used to account for the strong forward diffraction nature of the phase function of cloud particles to enhance computational accuracy. The parameterized radiative transfer equations with appropriate boundary conditions imposed are solved numerically by using an efficient successive over–relaxation method. For calculations of the broadband solar and thermal infrared fluxes in inhomogeneous cirrus cloud layers, a total of 121 wavelengths are used to cover the solar (0.2–5 μm) and thermal infrared (5–50 μm) spectra.

In the following, we illustrate the importance of 3D inhomogeneous cloud fields for the heating rates and fluxes typical of a meso–scale grid. We used the IWC and DE field constructed by Liou and Rao (1996) based on the optical depth and DE retrieved from the AVHRR data along with the balloon–borne replicator sounding data for the vertical profile of ice crystal size distributions. These data covered an area of 30 km by 20 km near Coffeyville, Kansas, on 5 December 1991 during the FIRE–II–IFO experiment. Fig. 3 shows the constructed IWC field in the horizontal plane and the latitude–height plane. The value of the IWC field varies from 0.5 to 5 mg m^{-3} in the horizontal and from 1 to 7 mg m^{-3} in the vertical, indicating that this cirrus cloud system was both horizontally and vertically inhomogeneous.

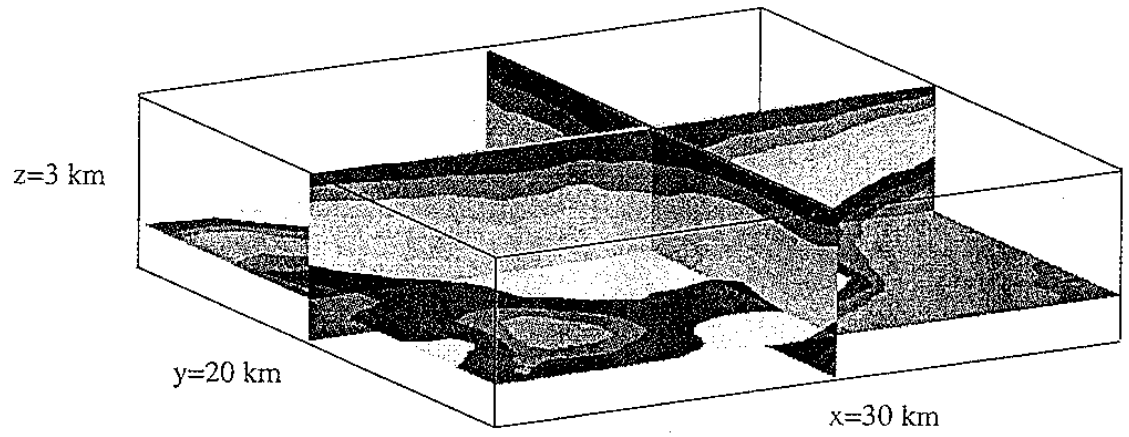

Fig. 3. IWC ($1.5x10^{-4}$ – $9x10^{-3}$ g m^{-3}) field constructed from AVHRR and balloon-borne replicator sounding data over the area near Coffeyville, Kansas, on 5 December 1991 in the xy, yz, and xz planes

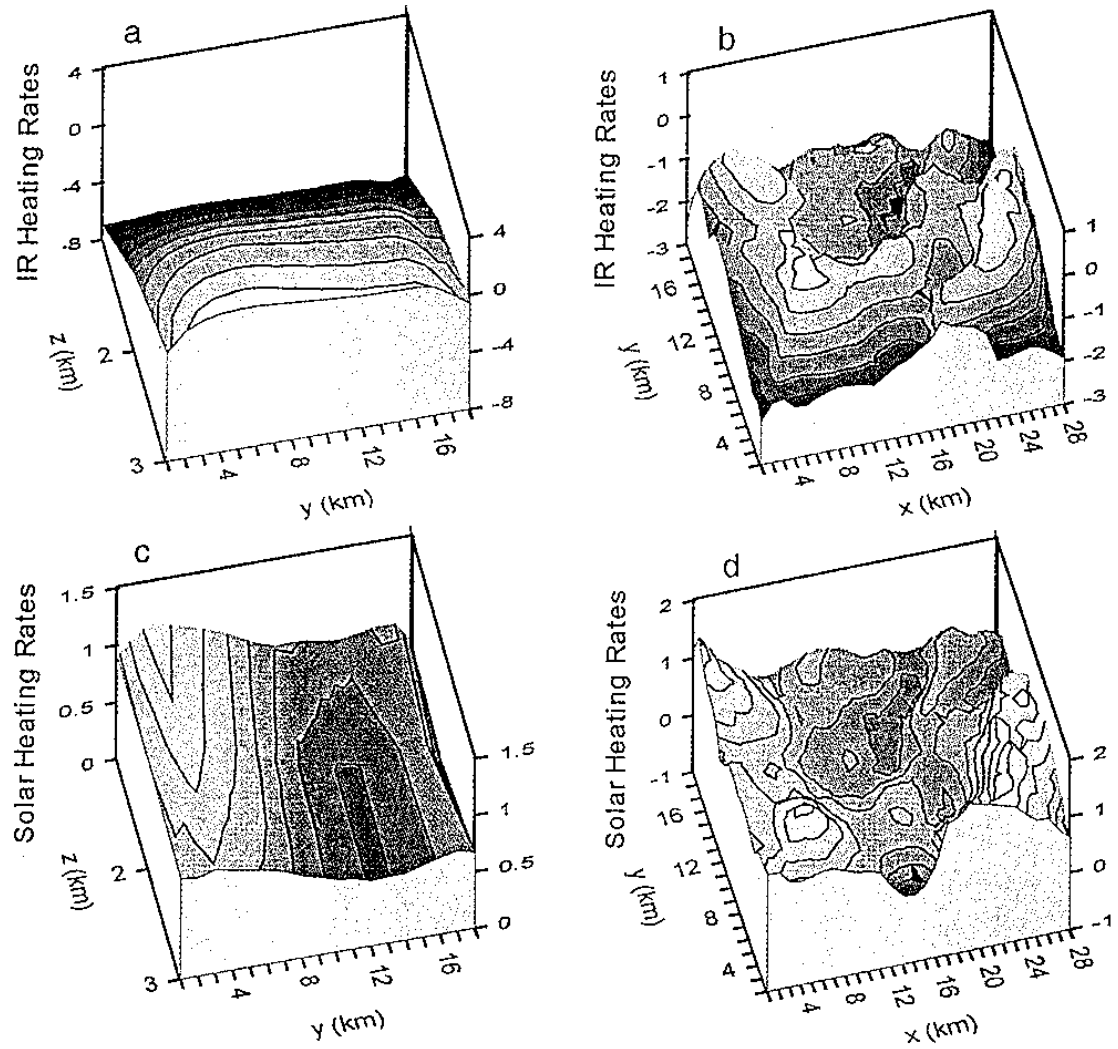

Fig. 4. 2D images of the differences in IR (a and b) and solar (c and d) heating rates (K day^{-1}) between inhomogeneous and homogeneous cirrus cloud layers. Results in (a) and (c) are presented in the latitude and height plane (averaged over longitude), while (b and (d) are shown in the horizontal plane (averaged over height).

Fig. 4 displays the differences in the averaged heating rates in the x–y and y–z planes between inhomogeneous and homogeneous clouds. For the homogeneous condition, mean single–scattering parameter values were used in the calculations. The solar zenith angle in this case is about 60°. In the x–y plane, the patterns correspond to the variabilities of the horizontal extinction coefficient (or IWC) field. More solar heating and IR warming are found in the area with larger extinction coefficients, while less solar heating and more IR cooling are shown in the area with smaller extinction coefficients. In the y–z plane, stronger IR cooling at the cloud top and slightly more IR warming at the bottom are displayed in the inhomogeneous case. This is associated with smaller extinction coefficients in the upper part of the cloud and larger values in the lower part of the inhomogeneous cirrus cloud. For solar radiation, more heating is found in the inhomogeneous case in the whole y–z plane.

On the basis of the preceding analysis, it is clear that the finite and inhomogeneous nature of clouds has a significant impact on the heating rate fields over a meso–scale grid as well as on the domain–averaged vertical heating profile. Many GCMs can now diagnose partial cloudiness for model layers. Maximum and random overlaps have been employed in the calculation of heating rates based on plane–parallel radiative transfer programs. Sensitivity of the finite and possible statistical distribution of cloudiness on domain–averaged heating rate profiles and its impact on climate simulations can be investigated by using the radiation parameterization program for 3D inhomogeneous clouds.

Finally, it should be emphasized that the cloud parameters derived from remote sensing of 3D cloud fields can be used to validate the liquid/ice water content predicted from contemporary GCMs, on the one hand, and on the other, to assist in the development of physically–based parameterizations for the predictions of cloud cover and cloud particle size.

Acknowledgements. Research reported in this paper has been supported by DOE Grant DE–FG03–00ER62904, NSF Grant ATM–9907924, and NASA Grant NAG5–7123.

REFERENCES

Fu, Q., and K. N. Liou, 1993: Parameterization of the radiative properties of cirrus clouds. *J. Atmos. Sci.*, **50**, 2008-2025.

Gu, Y., and K. N. Liou, 2000a: Interactions of radiation, microphysics, and turbulence in the evolution of cirrus clouds. *J. Atmos. Sci.*, **56** (in press).

Gu, Y., and K. N. Liou, 2000b: Radiation parameterization for three–dimensional inhomogeneous cirrus clouds: Application to climate research. *J. Climate* (submitted).

Liou, K. N., 1986: Influence of cirrus clouds on weather and climate processes: A global perspective. *Mon. Wea. Rev.*, **114**, 1167-1199.

Liou K. N., 1992: *Radiation and Cloud Processes in the Atmosphere: Theory, Observation, and Modelling*. Oxford University Press. 487 pp.

Liou, K. N., and N. X. Rao, 1996: Radiative transfer in cirrus clouds. Part IV: On cloud geometry, inhomogeneity, and absorption. *J. Atmos. Sci.*, **53**, 3046-3065.

Liou, K. N., and Q. Zheng, 1984: On the interaction of radiation, clouds, and dynamic processes in a general circulation model. *J. Atmos. Sci.*, **41**, 1513-1535.

Liou, K. N., P. Yang, Y. Takano, K. Sassen, T. Charlock, W. P. Arnott, 1998: On the radiative properties of contrail cirrus. *Geophys. Res. Lett.*, **25**, 1161-1164.

Mace, G., T. P. Ackerman, P. Minnis, D. F. Young, 1998: Cirrus layer microphysical properties derived from surface–based millimeter radar and infrared interferometer data. *J. Geophys. Res.*, **103**, 23207-23216.

Ou, S. C., K. N. Liou, and Co-authors, 1995: Remote sounding of cirrus cloud optical depths and ice crystal sizes from AVHRR data: Verification using FIRE–II–IFO composite measurements. *J. Appl. Sci.*, **52**, 4143-4158.

Ou, S. C., K. N. Liou, and B. A. Baum, 1996: Detection of multi–layer cirrus cloud systems using AVHRR data: Verification based on FIRE–II–IFO composite measurements. *J. Appl. Meteor.*, **35**, 178-191.

Ou, S.C., K. N. Liou, M. King, and S. C. Tsay, 1999: Remote sensing of cirrus clouds parameters based on a 0.63-3.7 μm radiance correlation technique applied to AVHRR data. *Geophys. Res. Lett.*, **26**, 2437-2440.

Randall, D. A., K. M. Xu, R. J. Somerville, and S. Iacobellis, 1996: Single–column models and cloud ensemble models as links between observations and climate models. *J. Climate*, **9**, 1683-1697.

Rolland, P., K. N. Liou, M. D. King, S. C. Tsay, and G. M. McFarquhar, 2000: Remote sensing of optical and microphysical properties of cirrus clouds using MODIS channels: Methodology and sensitivity to physical assumptions. *J. Geophys. Res.*, **105**, (May, in press).

Sassen, K., 1991: The polorization lidar technique for cloud research: A review and current assessment. *Bull. Amer. Meteor. Soc.*, **72**, 1848-1866.

Wylie, D. P., W. P. Menzel, H. M. Woolf, and K. I. Strabala, 1994: Four years of global cirrus cloud statistics using HIRS. *J. Climate*, **7**, 1972-1986.

Xu, K. M., and S. K. Krueger, 1991: Evaluation of cloudiness parameterizations using a cumulus ensemble model. *Mon. Wea. Rev.*, **119**, 342-367.